JOURNAL OF VIROLOGY, Dec. 1999, p. 10480–10488 Vol. 73, No. 12
0022-538X/99/$04.00+0

High Viral Load in the Cerebrospinal Fluid and Brain Correlates with Severity of Simian Immunodeficiency Virus Encephalitis

M. CHRISTINE ZINK,[1,2,3]* KALACHAR SURYANARAYANA,[4] JOSEPH L. MANKOWSKI,[1,2] ANDING SHEN,[1] MICHAEL PIATAK, JR.,[4] JEFFREY P. SPELMAN,[1] DARRYL L. CARTER,[1,2] ROBERT J. ADAMS,[1] JEFFREY D. LIFSON,[4] AND JANICE E. CLEMENTS[1,2,5]

Division of Comparative Medicine,[1] Department of Pathology,[2] and Department of Biochemistry and Molecular Biology,[5] Johns Hopkins University School of Medicine, and Department of Molecular Microbiology and Immunology, Johns Hopkins School of Hygiene and Public Health,[3] Baltimore, Maryland 21205, and Laboratory of Retroviral Pathogenesis, SAIC Frederick, National Cancer Institute-Frederick Cancer Research and Development Center, Frederick, Maryland 21702[4]

Received 28 April 1999/Accepted 24 August 1999

AIDS dementia and encephalitis are complications of AIDS occurring most frequently in patients who are immunosuppressed. The simian immunodeficiency virus (SIV) model used in this study was designed to reproducibly induce AIDS in macaques in order to examine the effects of a neurovirulent virus in this context. Pigtailed macaques (*Macaca nemestrina*) were coinoculated with an immunosuppressive virus (SIV/DeltaB670) and a neurovirulent molecularly cloned virus (SIV/17E-Fr), and more than 90% of the animals developed moderate to severe encephalitis within 6 months of inoculation. Viral load in plasma and cerebrospinal fluid (CSF) was examined longitudinally to onset of AIDS, and viral load was measured in brain tissue at necropsy to examine the relationship of systemic and central nervous system (CNS) viral replication to the development of encephalitis. In all animals, plasma viral load peaked at 10 to 14 days postinfection and remained high throughout infection with no correlation found between plasma viremia and SIV encephalitis. In contrast, persistent high levels of CSF viral RNA after the acute phase of infection correlated with the development of encephalitis. Although high levels of viral RNA were found in the CSF of all macaques (six of six) during the acute phase, this high level was maintained only in macaques developing SIV encephalitis (five of six). Furthermore, the level of both viral RNA and antigen in the brain correlated with the severity of the CNS lesions. The single animal in this group that did not have CNS lesions had no detectable viral RNA in any of the regions of the brain. The results substantiate the use of CSF viral load measurements in the postacute phase of SIV infection as a marker for encephalitis and CNS viral replication.

Human immunodeficiency virus (HIV) type 1-associated dementia affects approximately 25% of HIV-infected individuals, and pathological changes are seen in the brains of 70 to 90% of HIV-infected people (6, 24, 31). Despite this incidence of neurological disease and HIV lesions in the brain, the host and viral interactions that result in the development of HIV-associated dementia are not well understood. In individuals treated with highly active antiretroviral therapy, the incidence of AIDS and HIV-associated dementia has decreased (13, 15). However, the long-term effects of even transient virus replication in the central nervous system (CNS) are not clear, and treatment of HIV-infected individuals with highly active antiretroviral therapy is neither always effective nor universally available (11, 33). Thus, the role of HIV replication in the CNS and its correlation with the development of CNS disease and dementia remains an important and unresolved question.

Studies have shown that most individuals with HIV-associated dementia are in the terminal, immunosuppressive stages of disease, suggesting that intact immune responses may protect the CNS from dementia (30). Measurement of HIV RNA in plasma has been found to reflect the effectiveness of the host's immune responses, with plasma viral load serving as an important prognostic marker for the progression to AIDS (26). Given this association between dementia and immune suppression, a high viral load in plasma might be expected to be predictive for the development of dementia. However, studies conflict on whether or not this is the case (5, 7, 9, 12, 25).

A more direct way to measure the effectiveness of CNS immune responses in controlling HIV replication in the brain is to measure viral load in the cerebrospinal fluid (CSF). Recent studies using sensitive techniques to measure viral RNA show a correlation between viral load in CSF and brain and the presence of HIV-associated neurological disorders (5, 7, 10, 12, 25). However, viral gene products detected in the CSF may result from virus replication in the brain parenchyma, the meninges, or in trafficking infected mononuclear cells. In HIV-infected individuals, meningitis can occur independently of encephalitis. Thus, viral genotypes detected in the CSF may be derived from blood, since the CSF is produced as a filtrate of plasma, or from the brain, since fluid and trafficking cells from the brain parenchyma drain into the CSF via the Virchow-Robin spaces. In fact, two studies of viral genotypes in HIV have demonstrated that the viral genotypes isolated from the CSF are more similar to those in the periphery than those isolated from the brain parenchyma of the same individual (10, 21). Since different strains of virus may replicate in the brain and the CSF, viral load in CSF may not necessarily reflect viral replication in brain parenchyma.

Simian immunodeficiency virus (SIV) infection of macaques has been shown to recapitulate key features of HIV infection of the human CNS, including the development of encephalitis with characteristic histopathological changes and psychomotor impairment (27, 34). However, in most SIV models, both the

* Corresponding author. Mailing address: Retrovirus Laboratory, Traylor G-60, Johns Hopkins University School of Medicine, 720 Rutland Ave., Baltimore, MD 21205-2196. Phone: (410) 955-9770. Fax: (410) 955-9823. E-mail: mczink@mail.jhmi.edu.

incidence and time to onset of CNS disease are variable, greatly complicating the design and interpretation of studies. We therefore developed a model that achieves rapid and much more consistent development of SIV encephalitis, through coinoculation with two different SIV strains (34). In the present study, pigtailed macaques, a species more susceptible to SIV-induced CNS lesions than rhesus macaques (34), were coinoculated with immunosuppressive and neurovirulent viruses to recapitulate the association between immunosuppression and the development of AIDS dementia seen in humans. This rapid, reproducible model of SIV encephalitis and AIDS was used to examine the relationships between systemic and CNS viral replication and the development of lesions in the CNS. This is the first study that has performed longitudinal measurements of viral RNA in plasma and CSF from inoculation through terminal sacrifice and that has measured tissue-associated SIV RNA viral load in different brain regions. Viral loads in plasma, CSF, and brain were then compared with the presence and severity of SIV encephalitis to determine whether a correlation exists between viral load in various body compartments and SIV-induced neurological disease. There was no relationship between viral load in the plasma and the presence or severity of encephalitis. However, levels of viral RNA in the CSF during postacute infection correlated with the presence of CNS lesions. Further, levels of viral RNA and antigen in brain directly correlated with the presence and severity of CNS lesions.

MATERIALS AND METHODS

Viruses. SIV/DeltaB670 was originally obtained by coculturing lymph node tissue from SIV-infected monkey B670 with primary human phytohemagglutinin-stimulated peripheral blood mononuclear cells and was never passaged in cell lines. Macaques inoculated with this dualtropic virus swarm develop the full range of SIV-associated diseases, including immunosuppression, opportunistic infections, pneumonia, and encephalitis (3, 28). SIV/17E-Fr is a cloned recombinant, neurovirulent virus obtained by inserting the entire *env* and *nef* genes and the 3′ long terminal repeat of SIV/17E-Br, a virus isolated from the brain of a macaque with fulminant encephalitis, into the backbone of SIVmac239, the virus from which SIV/17E-Br had been derived by serial passage in rhesus macaques (2, 14, 23, 29). Recombinant virus stock was made by transfecting SIV/17E-Fr into CEMx174 cells.

Animals. In this study, only pigtailed macaques (*Macaca nemestrina*) were used, because in a previous study this species was found to develop CNS disease with a significantly higher frequency than rhesus macaques (34). Six macaques were intravenously inoculated with SIV/DeltaB670 (50 50% animal infectious doses [AID_{50}]) and SIV/17E-Fr (10,000 AID_{50}) as previously described but in an entirely independent group of animals (1, 34). The remaining three macaques were mock inoculated and served as virus-negative controls for quantitation of macrophage infiltration and pathology. Macaques were observed daily for clinical signs of illness such as inappetence, inactivity, or depression. Blood and CSF were sampled on postinoculation days 3, 7, 10, 14, and 28 and every 2 weeks thereafter. All manipulations were performed while the monkeys were anesthetized with ketamine-HCl (Parke-Davis, Morris Plains, N.J.). Five of six macaques were euthanized at 72 to 94 days postinfection (p.i.); one (no. 17850) died unexpectedly at 85 days p.i. Euthanasia was accomplished by anesthesia with ketamine-HCl followed by induction of deep anesthesia with pentobarbital and then perfusion with sterile phosphate-buffered saline to remove virus-containing blood from the vasculature. This was done to permit accurate quantitation of viral RNA in brain parenchyma.

$CD4^+$ cell counts. Complete blood counts with differentials were performed on every blood sample, and the absolute number of lymphocytes was determined by using a CellDyn 3200 hematology analyzer (Abbott). Mononuclear cells were separated on Percoll discontinuous gradients and labeled with fluorochrome-conjugated monoclonal antibodies (CD3, clone PR34 [Pharmingen]; CD4, clone Leu3a; CD8, clone Leu2 [Becton Dickinson]) to identify $CD4^+$ lymphocytes as previously described. Absolute $CD4^+$ cell counts were determined by multiplying the percentage of $CD4^+$ cells by the absolute lymphocyte count.

Measurement of binding and neutralizing antibody. To measure neutralizing antibody, plasma samples taken from the infected macaques at each time point were serially diluted fivefold with RPMI–10% fetal bovine serum in 96-well plates in a volume of 100 μl. All dilutions were done in quadruplicate; the assays were performed in duplicate. Diluted virus (100 μl, containing 5 to 10 50% tissue culture infective doses [$TCID_{50}$]) was added to each quadruplicate well. After incubating the plates at 37°C for 1 h, 10^4 CEMx174 cells were added to each well. Each dilution of virus without antibody was cultured with CEMx174 cells to determine the exact virus $TCID_{50}$ used in the neutralization assay. Plates were scored for the presence of virus-induced cytopathic effect after 7 to 10 days, and the 50% neutralization endpoint was calculated as previously described (8).

To measure binding antibody, a standard enzyme-linked immunosorbent assay was performed by using 96-well plates coated with recombinant SIV gp140. Plasma samples taken from the infected macaques at each time point were serially diluted twofold or fivefold and added to the coated wells. All dilutions were done in quadruplicate.

Viral RNA in plasma and CSF. Virion-associated SIV RNA in plasma and CSF were measured as an index of ongoing viral replication, using a real-time reverse transcription (RT)-PCR assay on an Applied Biosystems Prism 7700 Sequence Detection System, as previously described (18, 32). For each sample, three reactions were performed. Duplicate aliquots were separately reverse transcribed and amplified, and the amplification cycle during which a detectable PCR product was first observed (threshold cycle) was determined from real-time kinetic analysis of fluorescent product generation as a consequence of template-specific amplification (32). One reaction was processed and amplified without addition of reverse transcriptase. Nominal copy numbers for test samples were then automatically calculated by interpolation of the experimentally determined threshold cycle values onto a regression curve derived from control transcript standards, followed by normalization for the volume of the extracted plasma specimen.

Viral RNA in brain. For real-time RT-PCR quantitation of viral RNA in brain tissues, samples from four regions of the brain (basal ganglia, thalamus, parietal cortex, and cerebellum) were snap frozen in liquid nitrogen for RNA isolation. Quantitative measures of viral load in tissues are complex, ideally requiring internal controls for nucleic acid recovery and normalization for both RT conversion and PCR amplification efficiency. This is typically approached by using simultaneous quantitation of a viral target template and a cellular RNA species believed to be present at a relatively constant level per cell, regardless of cell type, differentiation, activation, or infection status. RNA was isolated from brain by a method that combines the use of the RNA STAT-60 Kit (Tel-Test "B", Inc.), followed by DNase treatment and final purification of the RNA with an RNeasy MiniKit from Qiagen. For both methods, the protocols supplied by the manufacturers were followed. Using 50 mg of tissue from brain, consistent recoveries of RNA were obtained.

Quantitation of SIV RNA in extracted brain tissue total RNA preparations was done with the same SIV *gag* region primers and probe and RT-PCR assay procedure described for plasma. This assay detects both cell-associated full-length viral transcripts and genomic RNA present in any tissue-associated virions. To normalize viral RNA copy number measurements, RNA copy numbers for two cellular transcripts were also determined for the same extracted RNA specimens used for SIV RNA determinations (32a). Total RNA was isolated from two control and six infected macaques. RNA copy numbers per microgram of total RNA were determined for transcripts encoding hypoxanthine phosphoribosyl transferase (HPRT) and phophobilinogen deaminase (PBGD) by real-time RT-PCR analysis on random-primed cDNA with the following primer and 3′-blocked probe combinations: for PBGD, forward primer (5′-CCAGCTTGC TCGGATACA-3′), reverse primer (5′-ACAACCAGGTCCACTTCATTC-3′), and probe (5′-*R*-CCACCACAGGGGACAAGATTCT-*O*-3′); and for HPRT, forward primer (5′-GTGGAAGATATAATTGACACTGCC-3′), reverse primer (5′-TCAAATCCAACAAAGTCTGGC-3′), and probe (5′-*R*-CAGACTTTGCT TTCCTTGGTCAGGCAG-*O*-3′); *R* indicates a 6-carboxy-fluorescein (FAM) group and *O* indicates a 6-carboxy-tetramethyl-rhodamine (TAMRA) group conjugated through a linker arm nucleotide linkage, as previously described (22).

Histopathology. Sections of the CNS, including frontal, parietal, temporal, and occipital cortex, basal ganglia, thalamus, midbrain, medulla, cerebellum, and cervical spinal cord were examined microscopically in a blinded fashion by two pathologists. To quantitate the severity of lesions, sections of frontal and parietal cortex, basal ganglia, thalamus, midbrain, and cerebellum were each given numerical scores of 1 (mild), 2 (moderate), or 3 (severe) by using the following semiquantitative system. Sections with more than 30 perivascular macrophage-rich cuffs were given a score of 3, sections with 10 to 30 perivascular cuffs were given a score of 2, and those with less than 10 perivascular cuffs were given a score of 1. The scores for all sections were totaled and divided by 6 (six regions were graded for each brain) to give a mean score (out of a maximum of 3) for severity of CNS lesions.

Quantitative immunohistochemical analysis. To detect viral gp41, a monoclonal antibody (kk41; AIDS Reagent Program) to the transmembrane portion of the SIVmac239 envelope that cross-reacts with SIV/17E-Fr and SIV/DeltaB670 was used. KP-1, which recognizes the macrophage marker CD68 (DAKO, Carpenteria, Calif.) was used to identify macrophages in the brain parenchyma. To ensure uniformity of staining essential for quantitative image analysis, all samples were stained by an Optimax Plus automated cell stainer (BioGenex, San Ramon, Calif.). Briefly, Streck-fixed, paraffin-embedded tissue sections were deparaffinized and rehydrated and then postfixed in Streck tissue fixative for 20 min. For antigen retrieval, tissues were rinsed in water and heated in a microwave in sodium citrate (0.01 M, pH 6.0) for 8 min. Endogenous peroxidase was quenched with 3% H_2O_2 in water for 10 min and then sections were blocked with buffered casein for 5 min. Primary antibody was applied to the tissues for 60 min at room temperature, the tissues were washed in wash buffer, and secondary biotinylated

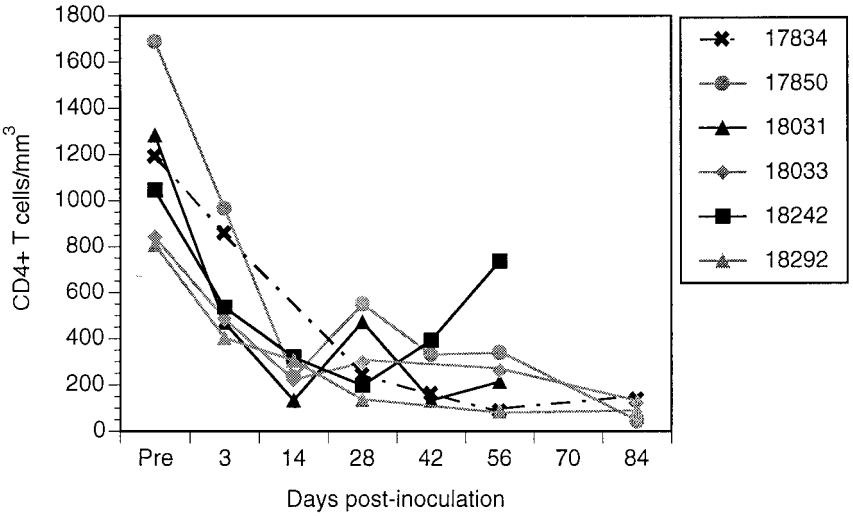

FIG. 1. Peripheral blood absolute $CD4^+$ lymphocyte counts of six macaques coinoculated with SIV/17E-Fr and SIV/DeltaB670. $CD4^+$ lymphocyte counts declined rapidly after inoculation and remained low throughout infection.

multilink antibody (BioGenex) was applied for 20 min. The tissues were washed again, and streptavidin-horseradish peroxidase was added for another 20 min. The sections were then washed, and diaminobenzidine tetrahydrochloride in buffer containing H_2O_2 was applied to the sections for 10 min. The sections were washed, dehydrated, and mounted. To permit accurate digital quantitation of signal, sections were not counterstained.

Quantitation of immunohistochemical staining on tissues was performed on 20 adjacent fields of tissue examined at a magnification of ×200 encompassing a 2.8-mm^2 area of subcortical white matter adjacent to the cingulate gyrus. Images were captured with a Sensys 2 digital camera (Photometrics, Tucson, Ariz.) and analyzed by using IP Lab imaging software (Scanalytics, Vienna, Va.). Images were binarized (each pixel converted to a value of 1 [positive] or 0 [negative]), and the total percent area occupied by positive pixels was calculated. This provides a quantitative measure of the total area occupied by positively stained cells or portions of cells in the area evaluated.

Statistical analysis. To determine whether there was a correlation between viral load and the severity of CNS lesions, the six macaques were ranked for level of viral RNA in plasma, CSF, and various regions of the brain for the percent area immunohistochemically stained for SIV gp41 or CD68 and for severity of CNS lesions. Spearman's rank correlation test was used to determine the degree of correlation between each measure of viral load and the severity of CNS lesions. Kendall's tau test was used to determine the significance of each correlation.

To examine the relationship between brain region and viral load, a random effect linear model was used. We specifically wanted to test whether viral load in the cerebellum was different than the average viral load in three other brain regions (basal ganglia, thalamus, and parietal cortex). A random effect model was chosen to correct for the correlation among measures taken from the same monkey. Data were log transformed to stabilize the variability across the range of the data.

RESULTS

A rapid, reproducible model of SIV AIDS and encephalitis was used in this study which employed coinoculation of pigtailed macaques with immunosuppressive and neurovirulent viruses. A previous study provided the basis for this model and showed that pigtailed macaques developed CNS lesions more frequently than rhesus macaques (34). Since humans infected with HIV develop AIDS encephalitis and dementia in the later stages of disease, when they are immunosuppressed, this animal model provides a parallel system in which to examine the important events associated with infection of the brain and the development of CNS lesions. This is the first study to measure viral load in the plasma and CSF longitudinally from acute infection to terminal AIDS and in the brain parenchyma at necropsy. Viral load was then compared with the presence and severity of CNS lesions to determine which measurements were predictive of SIV encephalitis.

Rapid decline in immune status of inoculated macaques. The immune status of the inoculated macaques was tracked by measuring $CD4^+$ lymphocyte counts twice a week during the first 2 weeks of infection and every 2 weeks thereafter. To control for variation in $CD4^+$ lymphocyte counts, three preinoculation measurements were taken to establish a baseline for each macaque. In all six inoculated macaques, lymphocyte counts declined rapidly during the first 2 weeks after inoculation and thereafter declined more gradually (Fig. 1). The average decline in $CD4^+$ lymphocytes for all six macaques throughout infection was 370 ± 177 cells per month. This decline in $CD4^+$ lymphocytes is more rapid than that seen in rhesus macaques inoculated with commonly used strains of SIV, such as SIVmac239 or SIVmac251.

Lack of humoral immune responses to virus. To examine whether the macaques developed humoral immune responses, plasma taken twice a week during the first 2 weeks of infection and every 2 weeks thereafter was tested for binding and neutralizing antibodies. The titers of binding antibodies in all macaques were very low throughout infection. Further, using a standard neutralization assay (described in Materials and Methods) in which 100 $TCID_{50}$ of virus was mixed with plasma (lowest dilution, fivefold), none of the six macaques produced any detectable neutralizing antibody at any time during infection. In contrast, macaques inoculated with SIV/17E-Fr (7a) or SIV/DeltaB670 (26a) alone developed high levels of neutralizing antibodies (50% neutralizing dose of 1,000 to 10,000) within 1 month of inoculation (unpublished observations). The inability to mount an effective immune response, rapidly declining $CD4^+$ lymphocyte counts, and rising viral loads are all characteristic of rapid progression in HIV-infected humans (4, 20).

SIV encephalitis in five of six macaques. Of the six infected macaques, three had severe (grade 2 to 3) and two had moderate (grade 1 to 2) pathological changes in the brain characteristic of encephalitis (Table 1). Typical of SIV encephalitis, the lesions were most severe in the subcortical white matter at the levels of the basal ganglia and thalamus. Pathological changes consisted of perivascular cuffs of macrophages, multinucleated giant cells and lymphocytes, diffuse hypercellularity of the neuropil, multifocal glial nodules, and isolated multinucleated giant cells scattered throughout the brain pa-

TABLE 1. Severity of pathological changes in different brain regions[a]

Macaque	Basal ganglia	Frontal cortex	Thalamus	Parietal cortex	Midbrain	Cerebellum
17834	0	0	0	0	0	0
18031	3	1	1	1	1	0
18242	2	2	2	2	2	1
18033	3	3	2	2	2	2
18292	2	3	2	3	2	2
17850	3	2	3	2	2	2

[a] Sections with more than 30 perivascular macrophage-rich cuffs were given a score of 3, sections with 10 to 30 perivascular cuffs were given a score of 2, and those with less than 10 perivascular cuffs were given a score of 1. The scores for all sections were totaled and divided by 6 (six regions were graded for each brain) to give the mean score (of a maximum of 3) for severity of CNS lesions shown in Table 2.

renchyma (Fig. 2). Macaque 17834 did not have any lesions in the brain or spinal cord.

Infiltration of macrophages in the CNS of the six inoculated macaques was quantified by image analysis of a standardized section of subcortical white matter immunohistochemically stained for the macrophage marker CD68. Macrophage staining in the three control macaques was used to quantitate the resident macrophage population. The method used for image analysis involved producing digital photographs of 20 adjacent fields of tissue examined at a magnification of ×200 encompassing a 2.8-mm^2 area of subcortical white matter adjacent to the cingulate gyrus. Captured images were binarized (each pixel converted to a value of 1 [positive] or 0 [negative]), and the total percent area occupied by positive pixels was calculated. The percent area occupied by positively stained pixels provided a quantitative measure of the total area occupied by cells or portions of cells in the area evaluated. When compared with the amount of CD68 staining in uninfected controls, this provided a quantitative numerical index of macrophage infiltration.

The percent area that stained positively for CD68 is shown in Table 2. When the macaques were ranked for CD68 expression and CNS lesion severity, there was a perfect correlation ($r = 1.0$). Thus, there was a significant correlation between the level of CD68 expression (a correlate of macrophage numbers) in the subcortical white matter and the severity of CNS lesions.

Viral RNA in plasma, CSF, and brain. To measure the level of virus replication in the periphery and the CNS of the infected macaques, viral RNA was quantified in plasma and CSF longitudinally and in brain tissue after sacrifice. Viral RNA in the plasma of inoculated macaques was measured by real-time RT-PCR (32). Viral load in plasma during acute infection reached peak levels (10^7 to 10^8 copy eq/ml) at 10 to 14 days after inoculation in all six infected macaques (Fig. 3). After a transient decrease of 0.3 to 1 log over the next 2 weeks, plasma viral RNA levels then either stabilized or rose, remaining in the range of 10^7 to 10^9 copy eq/ml for the subsequent duration of the study.

Viral RNA in the CSF was measured longitudinally during infection by the same method used for plasma. Viral RNA in CSF reached an initial peak (approximately 10^4 to 10^6 copy eq/ml) at 10 to 14 days after inoculation at the same time that viral RNA levels in plasma peaked (Fig. 4). From days 10 to 28 p.i., viral RNA in CSF decreased slightly or remained constant in five of six infected macaques, paralleling the slight decline of RNA observed in plasma. However, in macaque

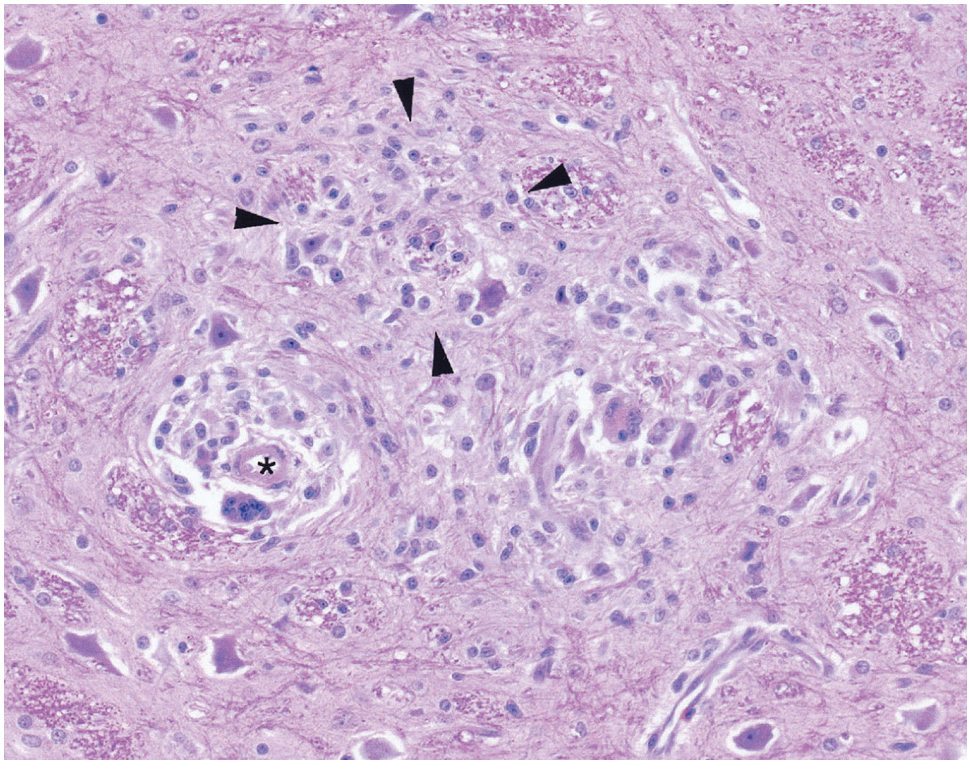

FIG. 2. Representative brain section from macaque 18033 at euthanasia. There were numerous perivascular cuffs (lumen of vessel is indicated by an asterisk) consisting of macrophages, multinucleated giant cells, and lymphocytes. Glial foci were also scattered throughout white matter (example indicated by arrowheads). These pathological changes are typical of those seen in the five macaques in this study with SIV encephalitis.

TABLE 2. CNS lesion severity, macrophage infiltration, and antigen expression in SIV-infected macaques

Macaque	Time of euthanasia (days p.i.)	CNS lesion severity mean score	CNS macrophage infiltration (% area)	CNS antigen expression (% area)	RNA in basal ganglia (10^6 copy eq/μg RNA)	RNA in basal ganglia (10^9 copy eq/g brain)
17834	92	0	0.17[a]	0	0	0
18031	87	1.2	0.27	0.03	2.8	1.4
18242	72	1.8	3.96	2.66	10.4	5.2
18033	94	2.3	4.26	0.46	3.8	1.9
18292	85	2.3	6.19	3.14	45.5	22.8
17850[b]	85	2.3	9.46	3.26	74.5	37.3

[a] The mean percent area occupied by resident macrophages in three uninfected macaques was 0.22%.
[b] Macaque 17850 died unexpectedly and thus was not perfused.

17834, which had no CNS lesions, viral load in CSF continued to decline, decreasing to below detectable levels by day 42 p.i. and increasing very slightly during terminal infection. In contrast, CSF viral RNA in the remaining five macaques increased steadily after 28 days p.i., reaching levels that matched those in plasma (10^7 to 10^8 copy eq/ml). These five macaques had moderate to severe CNS lesions and significant levels of viral antigen in the brain at necropsy. During terminal infection, there were 4 to 5 logs more viral RNA in the CSF of macaques with CNS lesions than in that of the macaque without CNS lesions. Thus, the presence of high levels of viral RNA in the CSF after the initial peak associated with primary infection correlated with the presence of CNS lesions at necropsy.

Viral RNA in the brain at necropsy was measured by real-time RT-PCR on RNA isolated from four different regions of the brain (basal ganglia, thalamus, parietal cortex, and cerebellum). These regions were chosen because the basal ganglia, thalamus, and parietal cortex are regions that most frequently contain virus-induced lesions, while the cerebellum is usually less severely affected. With the exception of macaque 17850, which died before perfusion could be performed, all SIV-inoculated animals and mock-inoculated controls were perfused with saline at necropsy so that tissues were free of virus-containing blood. This ensured that the viral RNA detected in the brain reflected virus present in the brain parenchyma and not in blood.

RNA copy numbers were determined for two cellular transcripts, HPRT and PBGD. As shown in Table 3, for both of these transcripts the values for measured copy equivalents per microgram of total RNA were relatively constant across different brain regions (within a factor of less than 2) and were not affected by SIV infection status. These observations indicate the appropriateness of normalization of tissue-associated SIV RNA copy numbers with values determined for either of these cellular transcripts in the same RNA specimen. SIV RNA levels in the brains from the infected macaques were normalized to both HPRT and PBGD to demonstrate these results (Fig. 5B and C).

High levels of SIV RNA were detected in the four regions of brain (basal ganglia, thalamus, parietal cortex, and cerebellum) examined in the five macaques (18031, 18242, 18033, 18292, and 17850) with moderate to severe CNS lesions (Fig. 5A). SIV RNA in the basal ganglia of the five macaques with SIV encephalitis ranged from 2.8×10^6 to 7.5×10^7 copy equivalents per microgram of RNA. These figures are equivalent to 1.4×10^9 to 3.8×10^{10} copies per gram of brain (Table 2). A statistically significant correlation was found between viral RNA in basal ganglia and CNS lesion severity ($r = 0.94$; $P = 0.008$). Since macaque 17850 was not perfused, we considered the possibility that viral RNA in plasma may have contributed to the high viral load detected in brain homogenates from this animal. Knowing the level of viral RNA in the plasma of macaque 17850 and that vasculature accounts for approximately 15% of the brain by volume (17), we therefore decreased the RNA levels detected in the basal ganglia of macaque 17850 to account for viral RNA in plasma within the

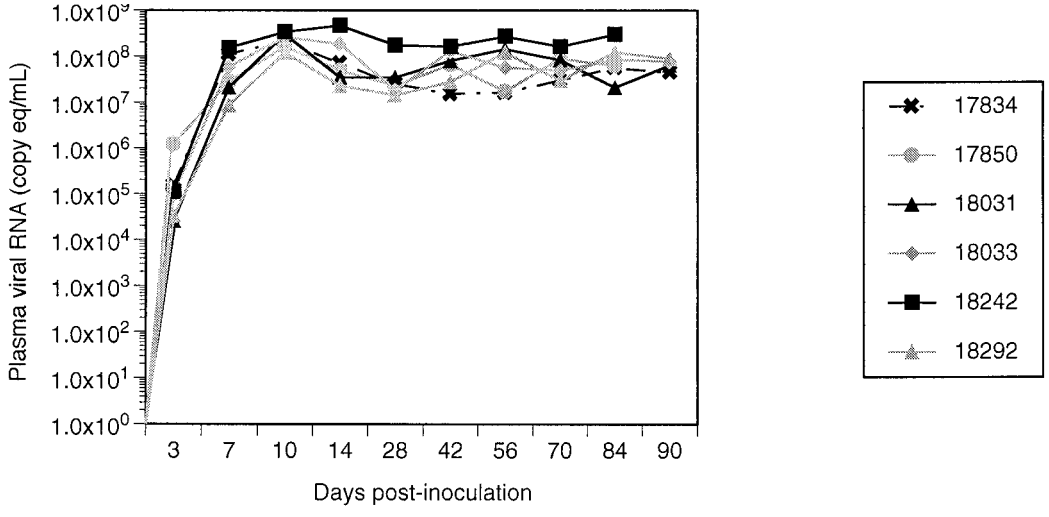

FIG. 3. Plasma viral RNA of six macaques coinoculated with SIV/17E-Fr and SIV/DeltaB670. Plasma viral RNA increased rapidly after inoculation in all six macaques and peaked at 10 days p.i. Thereafter, levels ranged between 10^7 and 10^9 copy eq/μl.

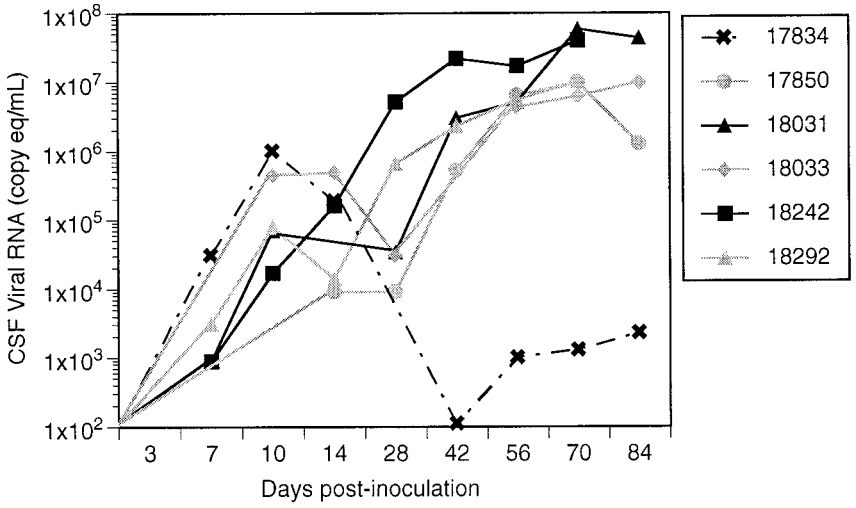

FIG. 4. CSF viral RNA of six macaques coinoculated with SIV/17E-Fr and SIV/DeltaB670. CSF viral RNA levels increased rapidly in all six macaques during acute infection, reaching a peak at 10 to 14 days p.i. CSF viral RNA levels in 17834, the macaque that did not develop CNS disease, then declined to very low levels. In contrast, CSF viral RNA in the five macaques that developed CNS disease remained the same or declined only slightly until 28 days p.i., after which they increased to levels that were 4 to 5 logs higher than those of 17834.

vasculature of the brain. Using the adjusted data, the results of our statistical analysis were unchanged.

Results indicated that viral load in the cerebellum was significantly lower than the average viral load in the other three brain regions ($P = 0.0052$). Using the random effect linear model, we estimated that the log response in the cerebellum is 0.58 copy equivalents per microgram of RNA lower than the average log response in the other three brain regions (95% confidence interval, -0.96 to -0.20). This corresponds to a 74% decline in viral load (95% confidence interval, 38 to 89%). These results are consistent with the finding of less severe lesions in this region of the brain.

No viral RNA could be detected in the brain of macaque 17834 by RT-PCR (multiple samples were taken to preclude the possibility of sampling error) or by RT-PCR followed by nested PCR (data not shown), despite high levels of viral RNA (5×10^7 copy eq/ml) in plasma at the time of sacrifice. Thus, the perfusion of the brain was extremely efficient in removing virus-contaminated blood from tissues.

Quantitation of virus gp41 expression in the brain. To determine whether viral RNA expression was also reflected in the synthesis of viral proteins in the brain, expression of SIV gp41 was examined. Standardized sections of subcortical white matter at the level of the basal ganglia were immunohistochemically stained with a monoclonal antibody to gp41 and assessed by quantitative digital image analysis (Table 1). There was no staining for gp41 in the brain of macaque 17834, the animal without CNS lesions. In contrast, the other five macaques had gp41 staining that occupied from 0.46 to 3.26% of the total area measured (2.8 mm^2). There was a significant correlation between the level of viral antigen expression in the subcortical white matter and the severity of CNS lesions ($r = 0.94$; $P = 0.005$). Further, there was also a significant correlation between the levels of viral RNA and antigen in the brain at necropsy ($P = 0.005$).

DISCUSSION

This is the first study to measure SIV RNA in plasma and CSF longitudinally from acute infection to terminal AIDS and to correlate those findings with viral load in the brain and the development of CNS lesions. This study demonstrated that high levels of virion-associated RNA in the CSF, measured after the initial peak associated with primary infection, strongly correlated with the presence of encephalitis. Further, a strong correlation was demonstrated between viral load in the brain and the presence and severity of SIV encephalitis.

During acute infection, very high levels of viral RNA were present in the CSF of all infected macaques, regardless of whether those animals ultimately developed neurological lesions. In contrast, during terminal infection, CSF viral loads above 10^4 copy eq/μg of RNA were seen only in macaques with CNS lesions. These results are consistent with studies describing high levels of viral RNA in the CSF of HIV-infected individuals with encephalitis or dementia (5, 7, 10, 12, 25). Two to four logs of viral RNA have been detected in the CSF of

TABLE 3. Expression of PBGD and HPRT in brains of SIV-infected and uninfected macaques

Cellular transcript and infection status	Basal ganglia (10^6 copy eq/μg RNA)	Thalamus (10^6 copy eq/μg RNA)	Parietal cortex (10^6 copy eq/μg RNA)	Cerebellum (10^6 copy eq/μg RNA)
PBGD				
Infected ($n = 6$)	1.22 ± 0.61	1.28 ± 0.31	1.09 ± 0.52	0.87 ± 0.09
Uninfected ($n = 3$)	1.02 ± 0.22	1.59 ± 0.60	1.61 ± 0.26	0.95 ± 0.11
HPRT				
Infected ($n = 6$)	1.68 ± 0.50	2.13 ± 0.66	1.6 ± 0.98	1.61 ± 0.53
Uninfected ($n = 3$)	1.78 ± 0.67	2.58 ± 0.28	2.27 ± 1.07	1.66 ± 0.17

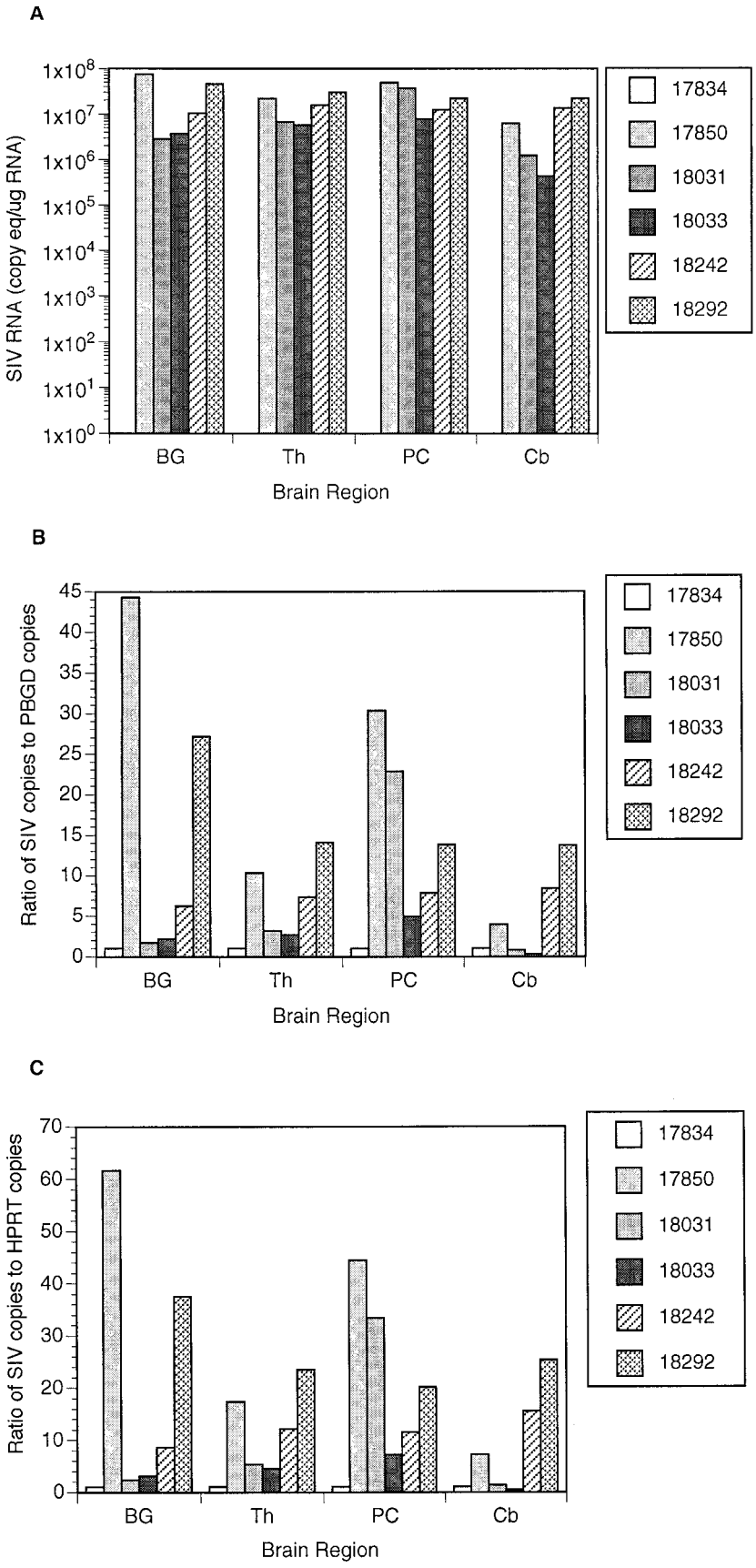

FIG. 5. Viral RNA in various regions of the brain. (A) SIV RNA copy equivalents per microgram of total RNA extracted from brain tissue homogenates. No viral RNA was detected in macaque 17834, whereas there were 10^6 to 10^8 copy eq/μg of total RNA in the five macaques with CNS lesions. (B) Ratio of SIV RNA copies to copies of PBGD in brain homogenates. (C) Ratio of SIV RNA copies to copies of HPRT in brain homogenates. BG, basal ganglia; Th, thalamus; PC, parietal cortex; Cb, cerebellum.

HIV-infected individuals without encephalitis or cognitive or motor changes (7, 12, 25). Our results suggest that such low levels of viral RNA in the CSF may be seen during primary infection, during early infection of the CNS, or in individuals without any CNS lesions. The data presented here suggest that viral load in CSF is a good surrogate marker for encephalitis during the postacute stages of infection. It is not yet clear whether high levels of viral RNA in the CSF during the clinically latent period are predictive of the development of neurological lesions. We were not able to assess viral load in that period since our model recapitulates rapid progression of AIDS. Hence, the macaques in this study never experienced a clinically latent period.

Of particular interest was the data demonstrating 10^6 copy eq/ml of CSF during acute infection in macaque 17834, which did not develop SIV encephalitis. CSF does not solely reflect virus replication in the brain parenchyma, but it may also contain virus produced in the meninges, virus from cells trafficking into the CNS, and virus from plasma that enters the brain through a compromised blood-brain barrier. It seems unlikely that such high levels of replication could occur acutely in the brain parenchyma and then be suppressed and leave no residual lesions 2 months later. Likewise, if the high levels of viral RNA in the CSF during acute infection were a result of a breakdown in the blood-brain barrier, macaque 17834 would be expected to show some CNS lesions or residual viral replication at euthanasia only 2 months later. The source of this initial peak of CSF RNA during the first 2 weeks of infection could reflect active virus replication in the meninges, since meningitis is frequently observed early in SIV infection. Another possibility is that the high CSF viral loads during acute infection represent extensive trafficking of infected cells from the blood, through the brain parenchyma, and out into the CSF. This would suggest that the brains of all infected individuals are exposed to virus during acute infection but that the virus becomes established and replicates long-term in only a subset of individuals.

Previous studies in both HIV-infected humans and SIV-infected macaques detected viral DNA in the brain of infected individuals with and without CNS disease (16, 19, 23). This viral DNA may be due to the trafficking of infected monocytes and lymphocytes into the CNS that leave the footprints of viral infection in those particular cells without the establishment of productive virus replication in the brain parenchyma. In studies of SIV strains that were macrophage-tropic but not neurovirulent, viral DNA was readily detected in the brain 2 to 3 years after inoculation, whereas viral RNA was not detected. In contrast, with SIV strains that cause CNS lesions, both viral DNA and RNA were detected in the brain at 1 to 2 years postinoculation (23). Thus, the development of CNS lesions appears to require the establishment of productive infection in the brain.

This study demonstrated a significant correlation between viral load (both RNA and gp41) in the basal ganglia and the severity of neurological lesions. When studying human tissues, the possibility exists that high levels of virus in the brain vasculature might artificially elevate viral load. This is of particular concern when using highly sensitive measures of viral load, such as real-time RT-PCR. The SIV-macaque model permits the flushing of virus-containing blood from the brain by saline perfusion. We were thus able to confirm that macaques with more extensive and severe CNS lesions also had higher viral RNA and gp41 levels in the brain.

This study also demonstrated a significant correlation between viral load (RNA or gp41) and macrophage infiltration. The majority of the infiltrating $CD68^+$ macrophages were not productively infected by SIV, as judged by immunohistochemical staining for gp41. The positive correlation between CNS viral load and degree of macrophage infiltration suggests that virus infection may signal the influx of cells, particularly macrophages into the brain. This may occur by direct virus-induced expression of chemokines, such as MCP-1, and/or indirectly through induction of chemokine-inducing cytokines. Those chemokines then signal the influx of inflammatory cells, some of which contain virus, thus setting up a vicious cycle of chemokine secretion and virus replication.

ACKNOWLEDGMENTS

We acknowledge the expert assistance of Maryann Brooks, Nicole Reed, Brandon Bullock, Tracy Miller, Li Li, Tom Parks, and Ken Anderson. Kelly Fox assisted with statistical analysis.

This study was funded by the following grants: NS35344, NS36911, HL53248, NS35751, NS38008, HL061962, and RR00116. This project was funded in part with federal funds from the National Cancer Institute, National Institutes of Health, under contract no. N01-CO-56000.

REFERENCES

1. **Amedee, A. M., N. Lacour, J. L. Gierman, L. N. Martin, J. E. Clements, R. Bohn, R. M. Harrison, and M. Murphey-Corb.** 1995. Genotypic selection of simian immunodeficiency virus in macaque infants infected transplacentally. J. Virol. **69:**7982–7990.
2. **Anderson, M. G., D. Hauer, D. P. Sharma, S. V. Joag, O. Narayan, M. C. Zink, and J. E. Clements.** 1993. Analysis of envelope changes acquired by SIVmac239 during neuroadaption in rhesus macaques. Virology **195:**616–626.
3. **Baskin, G. B., M. Murphey-Corb, L. N. Martin, K. F. Soike, F.-S. Hu, and D. Kuebler.** 1991. Lentivirus-induced pulmonary lesions in rhesus monkeys (*Macaca mulatta*) infected with simian immunodeficiency virus. Vet. Pathol. **28:**506–513.
4. **Borrow, P., H. Lewicki, B. H. Hahn, G. M. Shaw, and M. B. A. Oldstone.** 1994. Virus-specific $CD8^+$ cytotoxic T-lymphocyte activity associated with control of viremia in primary human immunodeficiency virus type 1 infection. J. Virol. **68:**6103–6110.
5. **Brew, B. J., L. Pemberton, P. Cunningham, and M. G. Law.** 1997. Levels of human immunodeficiency virus type 1 RNA in cerebrospinal fluid correlate with AIDS dementia stage. J. Infect. Dis. **175:**963–966.
6. **Budka, H.** 1991. Neuropathology of human immunodeficiency virus infection. Brain Pathol. **1:**163–175.
7. **Cinque, P., L. Vago, D. Ceresa, F. Mainini, M. R. Terreni, A. Vagani, W. Torri, S. Bossolasco, and A. Lazzarin.** 1998. Cerebrospinal fluid HIV-1 RNA levels: correlation with HIV encephalitis. AIDS **12:**389–394.

7a. **Clements, J. E.** Personal communication.

8. **Clements, J. E., R. C. Montelaro, M. C. Zink, A. M. Amedee, S. Miller, A. M. Trichel, B. Jagerski, D. Hauer, L. N. Martin, R. P. Bohm, et al.** 1995. Cross-protective immune responses induced in rhesus macaques by immunization with attenuated macrophage-tropic simian immunodeficiency virus. J. Virol. **69:**2737–2744.
9. **Dal Pan, G. J., H. Farzadegan, O. Selnes, D. R. Hoover, E. N. Miller, R. L. Skolasky, T. E. Nance-Sproson, and J. C. McArthur.** 1998. Sustained cognitive decline in HIV infection: relationship to CD4+ cell count, plasma viremia and p24 antigenemia. J. Neurovirol. **4:**95–99.
10. **Di Stefano, M., L. Monno, J. R. Fiore, G. Buccoliero, A. Appice, L. M. Perulli, G. Pastore, and G. Angarano.** 1998. Neurological disorders during HIV-1 infection correlate with viral load in cerebrospinal fluid but not with virus phenotype. AIDS **12:**737–743.
11. **Eggers, C. C., J. van Lunzen, T. Buhk, and H. J. Stellbrink.** 1999. HIV infection of the central nervous system is characterized by rapid turnover of viral RNA in cerebrospinal fluid. J. Acquir. Immune Defic. Syndr. Hum. Retrovirol. **20:**259–264.
12. **Ellis, R. J., K. Ksia, S. A. Spector, J. A. Nelson, R. K. Heaton, M. R. Wallace, I. Abramson, J. H. Atkinson, I. Grant, J. A. McCutchan, and HIV Neurobehavioral Research Center Group.** 1997. Cerebrospinal fluid human immunodeficiency virus type 1 RNA levels are elevated in neurocognitively impaired individuals with acquired immunodeficiency syndrome. Ann. Neurol. **42:**679–688.
13. **Ferrando, S., W. van Gorp, M. McElhiney, K. Goggin, M. Sewell, and J. Rabkin.** 1998. Highly active antiretroviral treatment in HIV infection: benefits for neuropsychological function. AIDS **12:**F65–F70.
14. **Flaherty, M., D. A. Hauer, J. L. Mankowski, M. C. Zink, and J. E. Clements.** 1997. Molecular and biological characterization of a neurovirulent molecular clone of SIV. J. Virol. **71:**5790–5798.
15. **Gendelman, H. E., J. Zheng, C. L. Coulter, A. Ghorpade, M. Che, M. Thylin, R. Rubocki, Y. Persidsky, F. Hahn, J. Reinhard, Jr., and S. Swindells.** 1998.

Suppression of inflammatory neurotoxins by highly active antiretroviral therapy in human immunodeficiency virus-associated dementia. J. Infect. Dis. **178:**1000–1007.
16. **Glass, J. D., H. Fedor, S. L. Wesselingh, and J. C. McArthur.** 1995. Immunocytochemical quantitation of human immunodeficiency virus in the brain: correlations with dementia. Ann. Neurol. **38:**755–762.
17. **Guyton, A. C.** 1991. Textbook of medical physiology, 8th ed. W. B. Saunders, Philadelphia, Pa.
18. **Hirsch, V. M., T. R. Fuerst, G. Sutter, M. W. Carroll, L. C. Yang, S. Goldstein, M. Piatak, W. R. Elkins, W. G. Alvord, D. C. Montefiori, B. Moss, and J. D. Lifson.** 1996. Patterns of viral replication correlate with outcome in simian immunodeficiency virus (SIV)-infected macaques: effect of prior immunization with a trivalent SIV vaccine in modified vaccinia virus Ankara. J. Virol. **70:**3741–3752.
19. **Johnson, R. T., J. D. Glass, J. C. McArthur, and B. W. Chesebro.** 1996. Quantitation of human immunodeficiency virus in brains of demented and nondemented patients with acquired immunodeficiency syndrome. Ann. Neurol. **39:**392–395.
20. **Koup, R. A., J. T. Safrit, Y. Cao, C. A. Andrews, G. McLeod, W. Borkowsky, C. Farthing, and D. D. Ho.** 1994. Temporal association of cellular immune responses with the initial control of viremia in primary human immunodeficiency virus type 1 syndrome. J. Virol. **68:**4650–4655.
21. **Koyanagi, Y., S. Miles, R. T. Mitsuyasu, J. E. Merrill, H. V. Vinters, and I. S. Chen.** 1987. Dual infection of the central nervous system by AIDS viruses with distinct cellular tropisms. Science **236:**819–822.
22. **Livak, K. J., S. J. Flood, J. Marmaro, W. Giusti, and K. Deetz.** 1995. Oligonucleotides with fluorescent dyes at opposite ends provide a quenched probe system useful for detecting PCR product and nucleic acid hybridization. PCR Methods Appl. **4:**357–362.
23. **Mankowski, J. L., M. A. Flaherty, J. P. Spelman, D. A. Hauer, P. J. Didier, A. Martin Amedee, M. Murphey-Corb, A. Munoz, J. E. Clements, and M. C. Zink.** 1997. Pathogenesis of simian immunodeficiency virus encephalitis: viral determinants of neurovirulence. J. Virol. **71:**6055–6060.
24. **McArthur, J. C., D. R. Hoover, H. Bacellar, E. N. Miller, B. A. Cohen, J. T. Becker, N. M. H. Graham, J. H. McArthur, O. A. Selnes, L. P. Jacobson, B. R. Visscher, M. Concha, and A. Saah.** 1993. Dementia in AIDS patients: incidence and risk factors. Neurology **43:**2245–2252.
25. **McArthur, J. C., D. R. McClernon, M. F. Cronin, T. E. Nance-Sproson, A. J. Saah, M. St. Clair, and E. R. Lanier.** 1997. Relationship between human immunodeficiency virus-associated dementia and viral load in cerebrospinal fluid and brain. Ann. Neurol. **42:**689–698.
26. **Mellors, J. W., A. Muñoz, J. V. Giorgi, J. B. Margolick, C. J. Tassoni, P. Gupta, L. A. Kingsley, J. A. Todd, A. J. Saah, R. Detels, J. P. Phair, and C. R. Rinaldo, Jr.** 1997. Plasma viral load and CD4+ lymphocytes as prognostic markers of HIV-1 infection. Ann. Intern Med. **126:**946–954.
26a. **Murphey-Corb, M.** Personal communication.
27. **Murray, E. A., D. M. Rausch, J. Lendvay, L. R. Sharer, and L. E. Eiden.** 1992. Cognitive and motor impairments associated with SIV infection in rhesus monkeys. Science **255:**1246–1249.
28. **Sharer, L. R., J. Michaels, M. Murphey-Corb, F.-S. Hu, D. J. Kuebler, L. N. Martin, and G. B. Baskin.** 1991. Serial pathogenesis study of SIV brain infection. J. Med. Primatol. **20:**211–217.
29. **Sharma, D. P., M. C. Zink, M. Anderson, R. Adams, J. E. Clements, S. V. Joag, and O. Narayan.** 1992. Derivation of neurotropic simian immunodeficiency virus from exclusively lymphocytetropic parental virus: pathogenesis of infection in macaques. J. Virol. **66:**3550–3556.
30. **Soontornniyomkij, V., J. A. Nieto-Rodriguez, A. J. Martinez, L. A. Kingsley, C. L. Achim, and C. A. Wiley.** 1998. Brain HIV burden and length of survival after AIDS diagnosis. Clin. Neuropathol. **17:**95–99.
31. **Spencer, D. C., and R. W. Price.** 1992. Human immunodeficiency virus and the central nervous system. Annu. Rev. Microbiol. **46:**655–693.
32. **Suryanarayana, K., T. A. Wiltrout, G. M. Vasquez, V. M. Hirsch, and J. D. Lifson.** 1998. Plasma SIV RNA viral load determination by real-time quantification of product generation in reverse transcriptase-polymerase chain reaction. AIDS Res. Hum. Retroviruses **14:**183–189.
32a. **Suryanarayana, K., et al.** Unpublished data.
33. **Wit, F. W., R. van Leeuwen, G. J. Weverling, S. Jurriaans, K. Nauta, R. Steingrover, J. Schuijtemaker, X. Eyssen, D. Fortuin, M. Weeda, F. de Wolf, P. Reiss, S. A. Danner, and J. M. Lange.** 1999. Outcome and predictors of failure of highly active antiretroviral therapy: one-year follow-up of a cohort of human immunodeficiency virus type 1-infected persons. J. Infect. Dis. **179:**790–798.
34. **Zink, M. C., A. M. Amedee, J. L. Mankowski, L. Craig, P. Didier, D. L. Carter, A. Munoz, M. Murphey-Corb, and J. E. Clements.** 1997. Pathogenesis of SIV encephalitis. Selection and replication of neurovirulent SIV. Am. J. Pathol. **151:**793–803.